

# Dependence of Electroweak Parameters on the Definition of the Top-Quark Mass

BERND A. KNieHL\*

Theoretical Physics Department, Fermi National Accelerator Laboratory,  
P.O. Box 500, Batavia, IL 60510, USA

## Abstract

The QCD corrections to electroweak parameters depend on the renormalization scheme and scales used to define the top-quark mass. We analyze these dependences for the  $W$ -boson mass predicted via  $\Delta r$  to  $\mathcal{O}(\alpha\alpha_s)$  and  $\mathcal{O}(\alpha\alpha_s^2)$  in the on-shell and  $\overline{\text{MS}}$  schemes. These variations provide us with a hint on the magnitude of the unknown higher-order QCD effects and contribute to the theoretical error of the prediction.

PACS numbers: 12.15.-y, 11.15.Me, 12.15.Lk, 14.65.Ha

## 1 Introduction

It is well known that strong-interactions effects on the vacuum-polarization functions of the electroweak gauge bosons play a significant rôle in present and future high-precision tests of the standard model (SM) [1,2,3,4]. In perturbative calculations to  $\mathcal{O}(\alpha\alpha_s)$  [5,6,7,8], these effects arise from the type of two-loop diagrams where one virtual gluon is exchanged within a quark loop inserted into an electroweak-gauge-boson line. Since the top quark is by far the heaviest established elementary particle, with a pole mass of  $M_t = (180 \pm 12)$  GeV [9], the leading high- $M_t$  terms, of  $\mathcal{O}(G_F M_t^2)$ , are particularly important. As for oblique corrections, *i. e.*, those which arise from the gauge-boson vacuum polarizations, these terms together with their quantum-chromodynamical (QCD) corrections are all concentrated in  $\Delta\rho = 1 - 1/\rho$ , where  $\rho$  is the familiar parameter introduced in Ref. [10]. The leading-order QCD corrections to  $\Delta\rho$  have been known for several years [6,7]; those of next-to-leading order have recently

---

\*Permanent address: Max-Planck-Institut für Physik, Werner-Heisenberg-Institut, Föhringer Ring 6, 80805 Munich, Germany.

been calculated [11] and found to be relatively large, having indeed a non-negligible impact on ongoing precision tests of the SM. It is of great phenomenological interest to estimate the residual theoretical uncertainty of the QCD corrections to  $\Delta\rho$  and other basic electroweak parameters such as  $\Delta r$  [12]. This is the motivation for the present paper.

QCD-improved analyses of electroweak parameters [1,2,3,4,5,6,7,8] are usually carried out using the pole definition of the top-quark mass. This directly corresponds to the mass parameter which is presently being extracted with the Fermilab Tevatron [9] and will be with the CERN Large Hadron Collider (LHC) and future  $e^+e^-$  linear colliders, since, in the propagation of the  $t$  and  $\bar{t}$  quarks between their production and decay vertices, configurations near their mass shells are kinematically favoured. As a matter of principle, however, this mass convention is arbitrary, and we might as well adopt another one. For, if all orders of the perturbation expansion were taken into account, the final result should not depend on the selected scheme. Yet, this no longer holds true if the perturbation series is truncated. In general, the finite-order results also depend on the renormalization scales of the quark masses. It is generally believed that the scheme and typical scale variations may be used to estimate the theoretical uncertainty due to the unknown higher-order corrections.

In this paper, we shall pay special attention to  $\Delta r$  [12], which parameterizes the non-photon corrections to the muon lifetime and allows us to indirectly determine the  $W$ -boson mass for given values of the top-quark and Higgs-boson masses. Using two popular definitions of quark mass in QCD, namely the pole mass and the mass of the modified minimal-subtraction ( $\overline{\text{MS}}$ ) scheme [13], we shall quantitatively analyze the scheme and scale dependences of the  $M_W$  prediction at next-to-leading order in QCD, and so estimate the residual theoretical error on  $M_W$  from QCD sources. Our evaluation of  $\Delta r$  will make full use of the present knowledge of higher-order corrections, so that the extracted  $M_W$  values should be reliable within the quoted errors. Confrontation of these values with the future high-precision measurements of  $M_W$  at the Tevatron and the CERN Large Electron-Positron Collider (LEP2), in connection with a reduced error on  $M_t$ , will allow us to pin down the mass of the SM Higgs boson and to facilitate the search for it.

At this point, a few comments on the so-called  $t\bar{t}$  threshold effects [14,15] are in order. The study of these effects was an attempt to estimate the dominant higher-order QCD corrections to  $\Delta\rho$  and other oblique electroweak parameters prior to their diagrammatical computation [11]. This approach was based on the assumption that the bulk of the QCD corrections arises from the ladder diagrams of multi-gluon exchange in the  $t\bar{t}$  system. The absorptive parts of these diagrams can be resummed in the non-relativistic approximation, producing a prominent enhancement of the  $t\bar{t}$  excitation curve in the threshold region along with a lowering of its onset. This treatment naturally takes into account the finite lifetime of the top quark as well. The real parts of the diagrams were then found via dispersion relations with subtractions derived from Ward identities. The fact that the explicit  $\mathcal{O}(\alpha_s^2 G_F M_t^2)$  calculation of  $\Delta\rho$  [11] nicely agrees with the rough  $t\bar{t}$ -threshold estimate [14]—in fact, it

comfortably lies within the errors quoted in Ref. [14]—may be viewed as some posterior justification of this method. However, the good agreement is, to some extent, fortuitous, since approximately 30% of the  $\mathcal{O}(\alpha_s^2 G_F M_t^2)$  correction is due to double-triangle diagrams [11], which are beyond the scope of Ref. [14]. Therefore and for other reasons given in Ref. [16], we shall take the point of view that, at the present time, the result of Ref. [11] represents the most reliable description of the QCD corrections to  $\Delta\rho$  beyond the leading order, and that the residual theoretical uncertainty may be assessed by analyzing scheme and scale variations.

This paper is organized as follows. In Section 2, we shall translate existing on-shell (OS) results for the gauge-boson vacuum polarizations in  $\mathcal{O}(\alpha\alpha_s)$  [7] to the  $\overline{\text{MS}}$  scheme of quark-mass renormalization. Furthermore, we shall take a look inside the renormalization-group (RG) structure of the QCD expansion of  $\Delta\rho$  to  $\mathcal{O}(\alpha_s^2 G_F M_t^2)$  [11]. In Section 3, we shall quantitatively analyze the scheme and scale dependences of the  $M_W$  value predicted from the analysis of  $\Delta r$  to leading and next-to-leading order in QCD. Our conclusions concerning the theoretical uncertainty in  $M_W$  of QCD origin are summarized in Section 4. The Appendix contains some general relations which may be used to implement the scale dependence of the QCD coupling and mass in the  $\overline{\text{MS}}$  scheme, and to switch between the  $\overline{\text{MS}}$  and OS schemes.

## 2 Formalism

We shall work in the electroweak OS renormalization scheme, which uses the fine-structure constant,  $\alpha$ , and the physical particle masses as basic parameters, and define  $c_w^2 = 1 - s_w^2 = M_W^2/M_Z^2$  [12,17]. Our analysis of  $\Delta r$  will be based on Refs. [1,2,3]. Following Refs. [2,3], we shall use the decomposition

$$\Delta r = \Delta\alpha - \frac{c_w^2}{s_w^2} \Delta\rho(1 - \Delta\alpha) + \Delta r_{rem}, \quad (1)$$

where  $\Delta\alpha$  embodies the contributions from the charged leptons and the first five quark flavours that drive the fine-structure constant from the Thomson limit to the  $Z$ -boson scale,  $\Delta\rho$  is the top-quark-induced shift in the  $\rho$  parameter [10] written with the Fermi constant,  $G_F$ , and  $\Delta r_{rem}$  is devoid of large logarithmic and power-like terms of fermionic origin. We would like to point out that, unlike  $\Delta\rho$ ,  $\Delta r_{rem}$  must be written in terms of  $\alpha$ , since it is via  $\Delta r$  that  $G_F$  is introduced into the SM [1,2,3,12]. To our knowledge, all existing analyses to  $\mathcal{O}(\alpha\alpha_s)$  of  $\Delta r$  and other oblique electroweak parameters with a non-trivial quark-mass dependence, *i.e.*, other than  $\Delta\rho$ , employ the pole definition of quark mass in QCD [1,2,3,4,5,6,7,8]. In the following, we shall describe how these calculations may be converted to other schemes of mass renormalization in QCD, in particular to the  $\overline{\text{MS}}$  scheme.

The relevant quantities in this context are the transverse gauge-boson vacuum polarizations induced by a pair of quarks, with pole masses  $M_1$  and  $M_2$ . Adopting the conventions

of Ref. [7], we may write the vector and axial-vector parts as

$$\Pi^{V,A}(s, M_1, M_2) = \frac{N_c}{3}\Pi_0^{V,A}(s, M_1, M_2) + a\frac{N_c C_F}{4}\Pi_1^{V,A}(s, M_1, M_2) + \mathcal{O}(a^2), \quad (2)$$

where  $s$  is the square of the external four-momentum,  $N_c = 3$ ,  $C_F = (N_c^2 - 1)/(2N_c) = 4/3$ , and  $a = \alpha_s/\pi$ . We shall employ dimensional regularization in  $n = 4 - 2\epsilon$  space-time dimensions and introduce a 't Hooft mass,  $\mu$ , to keep the coupling constants dimensionless. We shall suppress terms containing  $\gamma_E - \ln(4\pi)$ , where  $\gamma_E$  is Euler's constant. These terms may be retrieved by substituting  $\mu^2 \rightarrow 4\pi e^{-\gamma_E} \mu^2$ . In the  $\overline{\text{MS}}$  scheme [13], they are subtracted along with the poles in  $\epsilon$ . For later use, we list the lowest-order functions appearing in Eq. (2) [18]:

$$\begin{aligned} 4\pi^2\Pi_0^{V,A}(s, M_1, M_2) &= \left(\frac{1}{\epsilon} + \ln\frac{\mu^2}{M_1 M_2}\right) \left[s - \frac{3}{2}(M_1 \mp M_2)^2\right] \\ &+ \left[1 + \frac{1}{s} \left(-\frac{M_1^2 + M_2^2}{2} \pm 3M_1 M_2\right) - \frac{(M_1^2 - M_2^2)^2}{2s^2}\right] \sqrt{\lambda} \operatorname{arcosh} \frac{M_1^2 + M_2^2 - s}{2M_1 M_2} \\ &+ \frac{M_1^2 - M_2^2}{2s} \left[\frac{(M_1^2 - M_2^2)^2}{2s} \mp 3M_1 M_2\right] \ln \frac{M_1^2}{M_2^2} + \frac{5}{3}s - M_1^2 - M_2^2 \pm 6M_1 M_2 \\ &- \frac{(M_1^2 - M_2^2)^2}{2s} + \mathcal{O}(\epsilon), \end{aligned} \quad (3)$$

where  $\lambda = [s - (M_1 + M_2)^2][s - (M_1 - M_2)^2]$ . Equation (3) is valid for  $s < (M_1 - M_2)^2$ . It may be analytically continued to other values of  $s$  by observing that  $s$  comes with an infinitesimal, positive imaginary part, *i.e.*,  $s \rightarrow s + i\epsilon$ . Specifically,

$$\begin{aligned} \sqrt{\lambda} \operatorname{arcosh} \frac{M_1^2 + M_2^2 - s}{2M_1 M_2} &= -\sqrt{-\lambda} \arccos \frac{M_1^2 + M_2^2 - s}{2M_1 M_2} \\ &= -\sqrt{\lambda} \left( \operatorname{arcosh} \frac{s - M_1^2 - M_2^2}{2M_1 M_2} - i\pi \right). \end{aligned} \quad (4)$$

The general formulae for  $\Pi_1^{V,A}(s, M_1, M_2)$  are somewhat lengthy [8]. Fortunately, the finite-mass effects in  $\mathcal{O}(\alpha\alpha_s)$  on the oblique electroweak parameters (with the well-known exception of  $\Delta\alpha$ ) due to the first five quark flavours are exceedingly small [7,8], so that, beyond  $\mathcal{O}(\alpha)$ , we may safely neglect all quark masses, except for  $M_t$ . In this approximation, the mass-dependent cases may be cast into the form [7]

$$\begin{aligned} \frac{\pi^2}{M^2}\Pi_1^V(s, M, M) &= RX_1 + V_1(R) + \mathcal{O}(\epsilon), \\ \frac{\pi^2}{M^2}\Pi_1^A(s, M, M) &= RX_1 + Y_1 + A_1(R) + \mathcal{O}(\epsilon), \end{aligned}$$

$$\frac{\pi^2}{M^2}\Pi_1^{V,A}(s, M, 0) = \frac{1}{4}(XX_1 + Y_1) + F_1(X) + \mathcal{O}(\epsilon), \quad (5)$$

where  $V_1$ ,  $A_1$ , and  $F_1$  are finite functions of  $R = (s/4M^2)$  and  $X = s/M^2$ , and [8,19]

$$\begin{aligned} X_1 &= \frac{1}{2\epsilon} + L - 4\zeta(3) + \frac{55}{12}, \\ Y_1 &= \frac{3}{2\epsilon^2} + \frac{1}{\epsilon} \left( 3L + \frac{11}{4} \right) + 3L^2 + \frac{11}{2}L + 6\zeta(3) + \frac{9}{2}\zeta(2) - \frac{11}{8}, \end{aligned} \quad (6)$$

with  $L = \ln(\mu^2/M^2)$ . Here,  $\zeta$  is Riemann's zeta function, with values  $\zeta(2) = \pi^2/6$  and  $\zeta(3) \approx 1.202\,057$ .

The quantities in Eq. (5) refer to the OS scheme, *i.e.*, they contain the contributions which emerge from the respective one-loop seed diagrams by inserting the OS mass counterterm,  $\delta M = m_0 - M$ , where  $m_0$  is the bare quark mass, in all possible ways. The resulting shifts in  $\Pi_1^{V,A}$  may conveniently be constructed from  $\Pi_0^{V,A}$  through the variation

$$a \frac{N_c C_F}{4} \delta \Pi_1^{V,A}(s, M_1, M_2) = \frac{N_c}{3} \sum_{i=1}^2 \delta M_i \frac{\partial}{\partial M_i} \Pi_0^{V,A}(s, M_1, M_2). \quad (7)$$

For later use, we list the OS mass counterterm [20]:

$$\begin{aligned} \frac{\delta M}{M} &= -a C_F \left( \frac{\mu^2 e^{\gamma_E}}{M^2} \right)^\epsilon \Gamma(1 + \epsilon) \frac{3 - 2\epsilon}{4\epsilon(1 - 2\epsilon)} + \mathcal{O}(a^2) \\ &= -a C_F \left[ \frac{3}{4\epsilon} + \frac{3}{4}L + 1 + \epsilon \left( \frac{3}{8}L^2 + L + \frac{3}{8}\zeta(2) + 2 \right) + \mathcal{O}(\epsilon^2) \right] + \mathcal{O}(a^2), \end{aligned} \quad (8)$$

where  $\Gamma$  is Euler's Gamma function and  $L$  is defined below Eq. (6).

In other mass renormalization schemes,  $m_0$  is differently split into the renormalized mass,  $m$ , and the counterterm,  $\delta m$ , *i.e.*,

$$m_0 = M + \delta M = m + \delta m, \quad (9)$$

where  $\delta m$  differs from  $\delta M$  by some finite amount. In general,  $m$  depends on the renormalization scale,  $\mu$ , and on the QCD gauge parameter. Of all possible schemes, the  $\overline{\text{MS}}$  scheme is singled out because there  $\delta m$  just collects the  $\epsilon$  poles in Eq. (8). Furthermore, the  $\overline{\text{MS}}$  mass is gauge independent, as is  $M$  [20]. We may translate Eq. (2) to some other scheme by replacing  $M_i$  with  $m_i$  and adjusting the mass counterterms. The latter generates the shift

$$a \frac{N_c C_F}{4} \Delta \Pi_1^{V,A}(s, m_1, m_2) = \frac{N_c}{3} \sum_{i=1}^2 (M_i - m_i) \frac{\partial}{\partial m_i} \Pi_0^{V,A}(s, m_1, m_2), \quad (10)$$

where we have used Eq. (9). Notice that Eq. (10) does not require knowledge of the  $\mathcal{O}(\epsilon)$  terms of  $\Pi_0^{V,A}$ .

In the following, we shall take  $m$  to be the  $\overline{\text{MS}}$  mass. From Eq. (8), we may read off that

$$M = m \left[ 1 + aC_F \left( \frac{3}{4}l + 1 \right) + \mathcal{O}(a^2) \right], \quad (11)$$

where  $l = \ln(\mu^2/m^2)$ . The  $\mathcal{O}(a^2)$  term of Eq. (11) is written out in Eq. (30). With the help of Eqs. (3), (10), and (11), we may now convert Eq. (5) to the  $\overline{\text{MS}}$  scheme. The resulting expressions emerge from Eq. (5) by replacing  $M$ ,  $R$ ,  $X$ ,  $X_1$ ,  $Y_1$ ,  $V_1(R)$ ,  $A_1(R)$ , and  $F_1(X)$  with  $m$ ,  $r = (s/4m^2)$ ,  $x = s/m^2$ ,

$$\begin{aligned} \overline{X}_1 &= \frac{1}{2\epsilon} + l - 4\zeta(3) + \frac{55}{12}, \\ \overline{Y}_1 &= \frac{3}{2\epsilon^2} - \frac{5}{4\epsilon} - \frac{3}{2}l^2 - \frac{5}{2}l + 6\zeta(3) + 3\zeta(2) - \frac{75}{8}, \\ \overline{V}_1(r) &= V_1(r) + (3l + 4) \left( -\frac{\arcsin \sqrt{r}}{r\sqrt{1/r-1}} + 1 \right), \\ \overline{A}_1(r) &= A_1(r) + (3l + 4) \left( 2\sqrt{\frac{1}{r}-1} \arcsin \sqrt{r} - 1 \right), \\ \overline{F}_1(x) &= F_1(x) + \frac{1}{4}(3l + 4) \left[ \left( 1 - \frac{1}{x^2} \right) \ln(1-x) - \frac{1}{x} \right], \end{aligned} \quad (12)$$

respectively, where  $l$  is defined below Eq. (11). The last three lines of Eq. (12) are valid for  $0 \leq r, x \leq 1$ , the range relevant for the evaluation of electroweak parameters. Expressions appropriate for other values of  $r$  and  $x$  may be obtained with ease by analytic continuation as described in Ref. [21]. The following special cases frequently occur in applications:

$$\begin{aligned} \overline{V}_1(0) &= V_1(0) = 0, \\ \overline{V}'_1(0) &= V'_1(0) - \frac{2}{3}(3l + 4), \\ \overline{A}_1(0) &= A_1(0) + 3l + 4, \\ \overline{F}_1(0) &= F_1(0) + \frac{1}{8}(3l + 4). \end{aligned} \quad (13)$$

In the remainder of this section, we shall discuss the incorporation of three-loop QCD corrections [11,22] in Eq. (1). In Ref. [11], the  $\mathcal{O}(\alpha_s^2 G_F M_t^2)$  term of  $\Delta\rho$  has been calculated using both the OS and  $\overline{\text{MS}}$  definitions of quark mass in QCD. In Ref. [22], the  $\mathcal{O}(\alpha\alpha_s^2)$  correction to  $\Delta r_{rem}$  has been expanded in powers of  $M_Z^2/M_t^2$ , and the first two terms of this expansion have been presented both in the OS and  $\overline{\text{MS}}$  schemes. It is instructive to rewrite

the results of Ref. [11] in such a way that the RG origin of the logarithmic terms as well as the interrelation between the OS and  $\overline{\text{MS}}$  versions are explicitly displayed. This may be achieved with the help of Eqs. (22) and (30) for  $n_f = 6$  active quark flavours and leads to

$$\begin{aligned}\Delta\rho &= N_c X_t \left[ 1 + a R_1 (1 + a \beta_0 L) + a^2 R_2 + \mathcal{O}(a^3) \right] \\ &\approx 3 X_t \left[ 1 - 2.859\,912\,a \left( 1 + \frac{7}{4} a L \right) - 14.594\,028\,a^2 + \mathcal{O}(a^3) \right],\end{aligned}\quad (14)$$

$$\begin{aligned}\Delta\bar{\rho} &= N_c x_t \left\{ 1 + a \left[ 2\gamma_0 l + r_1 \left( 1 + a(\beta_0 + 2\gamma_0)l \right) \right] + a^2 \left[ \gamma_0(\beta_0 + 2\gamma_0)l^2 + 2(-2\gamma_0^2 + \gamma_1)l + r_2 \right] \right. \\ &\quad \left. + \mathcal{O}(a^3) \right\} \\ &\approx 3 x_t \left\{ 1 + a \left[ 2l - 0.193\,245 \left( 1 + \frac{15}{4} a l \right) \right] + a^2 \left( \frac{15}{4} l^2 + \frac{11}{4} l - 3.969\,560 \right) + \mathcal{O}(a^3) \right\},\end{aligned}\quad (15)$$

with

$$\begin{aligned}r_1 &= R_1 + 2C_F, \\ r_2 &= R_2 + C_F(2R_1 - 4\gamma_0 + C_F) + 2K_0,\end{aligned}\quad (16)$$

where  $X_t = (G_F M_t^2 / 8\pi^2 \sqrt{2})$ ,  $x_t = (G_F m_t^2 / 8\pi^2 \sqrt{2})$ , and  $L$  and  $l$  are defined below Eqs. (6) and (11), respectively. The first three coefficients of the beta function and the quark-mass anomalous dimension of QCD are listed in Eqs. (20) and (21), respectively, and  $K_0$  is defined in Eq. (29). The genuine information on the QCD correction to  $\Delta\rho$  is carried by  $R_1$  [6,7] and  $R_2$  [11] or, equivalently, by  $r_1$  [23] and  $r_2$  [11].

In the OS scheme, all  $\mu$  dependence originates in the renormalization of  $a$ , while the  $\overline{\text{MS}}$  scheme has  $m$  as an additional source of  $\mu$  dependence. So far, we have used a common renormalization scale,  $\mu$ , for  $a$  and  $m$ . In the following, we shall abandon this restriction and distinguish between coupling and mass renormalization scales,  $\mu_c$  and  $\mu_m$ . We shall henceforth use the symbol  $\mu_c$  in the OS expressions. In order to disentangle  $\mu_c$  and  $\mu_m$  in the  $\overline{\text{MS}}$  formulae, we first replace  $\mu$  with  $\mu_m$  and then substitute

$$a(\mu_m) = a(\mu_c) \left[ 1 - a(\mu_c) \beta_0 \ln \frac{\mu_m^2}{\mu_c^2} + \mathcal{O}(a^2) \right],\quad (17)$$

which follows from Eq. (22). Finally, we expand the resulting expressions in powers of  $a(\mu_c)$  and truncate these expansions beyond the order under consideration.

In the next section, we shall estimate the QCD-related theoretical uncertainty in  $M_W$  by studying the scheme and scale dependences of the  $\Delta r$  analysis. In order for our estimate to be meaningful, we shall have to judiciously choose the central values and widths of the scale intervals. It is natural to define the central values of  $\mu_c$  and  $\mu_m$  in such a way that

there the radiative corrections are devoid of logarithmic terms. Looking at Eqs. (14) and (15), we are thus led to set  $\mu_c = \xi_c M_t$  in the OS scheme, and  $\mu_c = \xi_c \bar{\mu}_t$  and  $\mu_m = \xi_m \bar{\mu}_t$ , where  $\bar{\mu}_t = m_t(\bar{\mu}_t)$ , in the  $\overline{\text{MS}}$  scheme. Here,  $\xi_c$  and  $\xi_m$  are variable numbers of order unity. A closed expression for  $\bar{\mu}_t$  in terms of  $M_t$  may be found in Eq. (31).

### 3 Numerical analysis

We are now in a position to quantitatively explore the scheme and scale dependences of the  $M_W$  prediction on the basis of  $\Delta r$ . Our starting point is the OS analysis of Ref. [2], which includes the dominant corrections beyond one loop, of  $\mathcal{O}(\alpha_s)$  [7],  $\mathcal{O}(G_F^2 M_t^4)$  [24], and  $\mathcal{O}(G_F^2 M_W^2 M_H^2)$  [1,2,25]. Here, we extend this analysis to  $\mathcal{O}(\alpha_s^2)$  by accommodating the respective corrections to  $\Delta\rho$  [11] and  $\Delta r_{rem}$  [22] in Eq. (1). Furthermore, we update our input parameters according to Refs. [26,27,28,29]. In particular, we use the combined LEP1 value  $M_Z = 91.1887$  GeV [27], the value  $\Delta\alpha_{had}^{(5)} = 0.0280$  [28] for the hadronic contribution to  $\Delta\alpha$ , and the world average  $\alpha_s^{(5)}(M_Z) = 0.118$  [29]. For the purpose of studying the scheme and scale dependences of  $\Delta r$ , we may assume that  $M_H$ ,  $M_t$ , and  $\alpha_s^{(6)}(M_t)$  are precisely known. Unless stated otherwise, we choose  $M_H = 300$  GeV [27] and  $M_t = 180$  GeV [9]. We compute  $\alpha_s^{(6)}(M_t)$  at three loops in two steps. First, we scale  $\alpha_s^{(5)}(\mu_c)$  from  $\mu_c = M_Z$  to  $\mu_c = M_t$  via Eq. (23) with  $n_f = 5$ . Then, we cross the flavour threshold at  $\mu_c = M_t$  using the matching condition (32). For  $M_t = 180$  GeV, we so obtain  $\alpha_s^{(6)}(M_t) = 0.1071$ . In order for our findings concerning the scheme and scale dependences to be meaningful, it is crucial that we consistently evaluate  $\alpha_s^{(6)}(\mu)$ ,  $m_t(\mu)$ , and  $\bar{\mu}_t$  to the order that we consider at a time. For the analysis of  $\Delta r$  to  $\mathcal{O}(\alpha_s^2)$ , we first compute  $\alpha_s^{(6)}(\mu)$  using Eq. (23) for  $n_f = 6$  with the  $\mathcal{O}(\alpha_s^3)$  terms in the denominator omitted. Then, we insert this value together with  $\alpha_s^{(6)}(M_t)$  and  $m_t(M_t)$ , which we extract from Eq. (28), into Eq. (25) to obtain  $m_t(\mu)$ . We evaluate  $\bar{\mu}_t$  by means of Eq. (31). If we calculate  $\Delta r$  to  $\mathcal{O}(\alpha_s)$ , then we correspondingly discard the  $\mathcal{O}(\alpha_s^2)$  terms in Eqs. (23), (28), and (31) and employ Eq. (24) instead of Eq. (25).

In Table 1, we investigate the scheme dependence of the  $M_W$  prediction via  $\Delta r$  to  $\mathcal{O}(\alpha_s)$  and  $\mathcal{O}(\alpha_s^2)$  within the ranges  $160 \text{ GeV} \leq M_t \leq 210 \text{ GeV}$  and  $60 \text{ GeV} \leq M_H \leq 1 \text{ TeV}$ . For the time being, we suppress the logarithmic terms of RG origin by choosing  $\xi_c = \xi_m = 1$ . For this choice, the  $\overline{\text{MS}}$  values are always in excess of the the respective OS numbers, *i.e.*, the QCD corrections are less negative in the  $\overline{\text{MS}}$  scheme. In Fig. 1, we display this excess as a function of  $M_H$  for  $M_t = 168, 180, \text{ and } 192$  GeV [9] both in  $\mathcal{O}(\alpha_s)$  and  $\mathcal{O}(\alpha_s^2)$ . We observe that the scheme dependence increases both with  $M_t$  and  $M_H$ . For the  $M_t$  and  $M_H$  intervals considered in Table 1, it ranges from 4.7 to 13.2 MeV in  $\mathcal{O}(\alpha_s)$  and from 2.2 to 10.3 MeV in  $\mathcal{O}(\alpha_s^2)$ . As expected, it is significantly reduced as we pass from  $\mathcal{O}(\alpha_s)$  to  $\mathcal{O}(\alpha_s^2)$ . For  $M_t = 180$  GeV, the reduction amounts to 51% (28%) for  $M_H = 60$  GeV (1 TeV). In Table 1, we also list the values of  $\bar{\mu}_t$  in  $\mathcal{O}(\alpha_s)$  and  $\mathcal{O}(\alpha_s^2)$ . In  $\mathcal{O}(\alpha_s^2)$ , they lie by a roughly



Table 1:  $M_W$  predicted for various values of  $M_t$  and  $M_H$  via  $\Delta r$  to  $\mathcal{O}(\alpha\alpha_s)$  and  $\mathcal{O}(\alpha\alpha_s^2)$  in the OS and  $\overline{\text{MS}}$  schemes with  $\xi_c = \xi_m = 1$ . For reference, also the  $M_W$  values evaluated without perturbative QCD corrections are given. Also  $\bar{\mu}_t$  is listed. All masses are given in GeV.

$M_t$	$\bar{\mu}_t$		$M_H$	$M_W$				
	$\mathcal{O}(\alpha_s)$	$\mathcal{O}(\alpha_s^2)$		w/o QCD	$\mathcal{O}(\alpha_s)$ OS	$\mathcal{O}(\alpha_s)$ $\overline{\text{MS}}$	$\mathcal{O}(\alpha_s^2)$ OS	$\mathcal{O}(\alpha_s^2)$ $\overline{\text{MS}}$
160	153.1	151.5	60	80.398	80.343	80.348	80.332	80.335
			300	80.295	80.240	80.245	80.229	80.232
			1000	80.199	80.143	80.150	80.133	80.137
170	162.7	161.1	60	80.468	80.407	80.413	80.396	80.398
			300	80.362	80.302	80.309	80.290	80.294
			1000	80.265	80.204	80.212	80.193	80.198
180	172.3	170.6	60	80.540	80.474	80.480	80.462	80.464
			300	80.433	80.367	80.374	80.354	80.359
			1000	80.334	80.268	80.276	80.255	80.261
190	182.0	180.2	60	80.616	80.544	80.550	80.530	80.534
			300	80.506	80.434	80.443	80.420	80.426
			1000	80.405	80.333	80.343	80.319	80.327
200	191.6	189.7	60	80.695	80.616	80.624	80.602	80.605
			300	80.582	80.504	80.513	80.489	80.496
			1000	80.479	80.400	80.412	80.386	80.395
210	201.2	199.3	60	80.777	80.692	80.700	80.676	80.680
			300	80.661	80.576	80.587	80.560	80.568
			1000	80.555	80.470	80.483	80.454	80.465

constant amount of 10 GeV below the respective  $M_t$  values. This may also be seen from Eq. (31), where, in the case of top, the coefficients of  $\alpha_s(M_t)/\pi$  and  $[\alpha_s(M_t)/\pi]^2$  are  $-4/3$  and  $-6.458784$ , respectively. To assess the significance of the scheme and scale dependences relative to the overall QCD effect on  $M_W$ , we also include in Table 1 the respective  $M_W$  values evaluated with the (perturbative) QCD corrections switched off. Of course, we cannot reliably eliminate the intrinsic non-perturbative QCD corrections contained in  $\Delta\alpha_{had}^{(5)}$ , *i.e.*, without introducing a significant dependence on the poorly-known light-quark masses.

In the remainder of this section, we shall stick to the central values  $M_t = 180$  GeV and  $M_H = 300$  GeV, and consider scale variations with  $1/8 \leq \xi_c, \xi_m \leq 8$ . In Table 2 and Fig. 2, we study the  $\mu_c$  dependence of  $M_W$  to  $\mathcal{O}(\alpha\alpha_s)$  and  $\mathcal{O}(\alpha\alpha_s^2)$  in the OS scheme. Obviously, the scale dependence is dramatically reduced, from 33.7 MeV to 11.1 MeV, *i.e.* by 67%, if the  $\mathcal{O}(\alpha\alpha_s^2)$  correction is taken into account. This should be compared with the shifts in  $M_W$

Table 2:  $M_W$  (in GeV) predicted for  $M_t = 180$  GeV and  $M_H = 300$  GeV via  $\Delta r$  to  $\mathcal{O}(\alpha\alpha_s)$  and  $\mathcal{O}(\alpha\alpha_s^2)$  in the OS scheme with  $\xi_c$  variable.

$\xi_c$	$M_W$ [GeV]	
	$\mathcal{O}(\alpha\alpha_s)$	$\mathcal{O}(\alpha\alpha_s^2)$
1/8	80.346	80.351
1/4	80.354	80.351
1/2	80.361	80.352
1	80.367	80.354
2	80.372	80.357
4	80.376	80.359
8	80.379	80.362

induced by the QCD corrections to  $\mathcal{O}(\alpha\alpha_s)$  and  $\mathcal{O}(\alpha\alpha_s^2)$  for  $\mu_c = M_t$ , which are  $-66.1$  MeV and  $-78.6$  MeV, respectively, as may be seen from Table 1. It is interesting to note that 2.4 MeV, *i.e.*, 19%, of the difference between the  $\mathcal{O}(\alpha\alpha_s)$  and  $\mathcal{O}(\alpha\alpha_s^2)$  evaluations of  $M_W$  is due to the three-loop correction to  $\Delta r_{rem}$  [22]. The  $\mathcal{O}(\alpha\alpha_s^2)$  evaluation exhibits a local minimum at  $\xi_c = 0.176$ . This is the point advocated by the principle of minimal sensitivity (PMS) [30]. The  $\mathcal{O}(\alpha\alpha_s)$  and  $\mathcal{O}(\alpha\alpha_s^2)$  curves cross over at  $\xi_c = 0.183$ , the point of fastest apparent convergence (FAC) [31]. In the OS analysis of  $\Delta\rho$  to  $\mathcal{O}(\alpha_s^2 G_F M_t^2)$  with  $n_f = 5$ , these points occur at  $\xi_c = 0.224$  and  $\xi_c = 0.264$ , respectively [32]. We note in passing that the application of the Brodsky–Lepage–Mackenzie (BLM) [33] scale-setting criterion to  $\Delta\rho$  leads to  $\xi_c = 0.154$  [11,32,34], which had been anticipated in the pioneering work of Ref. [34] prior to the advent of the  $\mathcal{O}(\alpha_s^2 G_F M_t^2)$  calculation of  $\Delta\rho$  [11].

In Table 3 and Fig. 3, we investigate how the  $\mathcal{O}(\alpha\alpha_s)$  and  $\mathcal{O}(\alpha\alpha_s^2)$  calculations of  $M_W$  in the  $\overline{\text{MS}}$  scheme depend on  $\mu_c$  and  $\mu_m$ . We notice that the  $\mu_c$  dependence is rather feeble for  $\mu_m \approx \bar{\mu}_t$ . This may be understood by observing that the coefficient of  $\alpha_s(\mu_c)/\pi$  in the QCD expansion of  $\Delta\bar{\rho}$  in Eq. (15) is then greatly suppressed [23]. In Fig. 3, the points of minimal sensitivity, *i.e.*, with zero tangents, are marked with “ $x$ .” They are saddle points and gathered in a small strip around  $\mu_m = \bar{\mu}_t$ . Their  $(\xi_c, \xi_m)$  coordinates are  $(2.732, 1.024)$  in  $\mathcal{O}(\alpha\alpha_s)$  and  $(0.133, 0.853)$  and  $(7.127, 1.147)$  in  $\mathcal{O}(\alpha\alpha_s^2)$ . For fixed  $\xi_c < 1$ , the  $\mathcal{O}(\alpha\alpha_s)$  value of  $M_W$  varies quite strongly with  $\xi_m$ , by 185.4 MeV for  $\xi_c = 1/8$ . This has to be compared with the shift in  $M_W$  due to the  $\mathcal{O}(\alpha\alpha_s)$  correction for  $\xi_c = \xi_m = 1$ , which only is 58.6 MeV in size (see Table 1). Of course, such an extreme variation cannot be interpreted as the uncertainty due to the neglect of higher-order QCD corrections. This rather tells us that our choice of the  $\xi_m$  interval width is not judicious in this case. Fortunately, the  $\mathcal{O}(\alpha\alpha_s^2)$  calculation is much more stable under scale variations. Here, the overall fluctuation is just 25.7 MeV, while the QCD-induced shift in  $M_W$  for  $\xi_c = \xi_m = 1$  is 73.8 MeV in magnitude

Table 3:  $M_W$  (in GeV) predicted for  $M_t = 180$  GeV and  $M_H = 300$  GeV via  $\Delta r$  to  $\mathcal{O}(\alpha\alpha_s)$  (upper entries) and  $\mathcal{O}(\alpha\alpha_s^2)$  (lower entries) in the  $\overline{\text{MS}}$  scheme with  $\xi_c$  and  $\xi_m$  variable.

$\xi_c \backslash \xi_m$	1/8	1/4	1/2	1	2	4	8
1/8	80.256 80.365	80.304 80.360	80.343 80.357	80.374 80.357	80.399 80.357	80.421 80.357	80.441 80.357
1/4	80.290 80.349	80.325 80.352	80.352 80.355	80.374 80.358	80.392 80.361	80.407 80.363	80.421 80.366
1/2	80.318 80.343	80.342 80.349	80.360 80.354	80.374 80.358	80.386 80.362	80.395 80.366	80.404 80.369
1	80.342 80.344	80.356 80.350	80.366 80.355	80.374 80.359	80.380 80.363	80.386 80.366	80.390 80.368
2	80.362 80.347	80.368 80.352	80.372 80.356	80.374 80.359	80.376 80.362	80.377 80.364	80.378 80.366
4	80.379 80.353	80.378 80.356	80.377 80.358	80.375 80.360	80.372 80.361	80.370 80.362	80.369 80.363
8	80.394 80.360	80.387 80.360	80.381 80.360	80.375 80.360	80.369 80.360	80.364 80.360	80.360 80.359

(see Table 1). However, this variation is still approximately 2.3 times as large as the one in the corresponding OS calculation.

Since it is hard to extract precise numbers from the contour plots in Fig. 3, we list in Table 4 the maximum deviations of the  $\overline{\text{MS}}$  evaluations of  $M_W$  to  $\mathcal{O}(\alpha\alpha_s)$  and  $\mathcal{O}(\alpha\alpha_s^2)$  within the variable range  $1/\xi_{max} \leq \xi_c, \xi_m \leq \xi_{max}$  from the respective values for  $\xi_c = \xi_m = 1$ . For completeness, we also list the corresponding numbers for the OS analyses to  $\mathcal{O}(\alpha\alpha_s)$  and  $\mathcal{O}(\alpha\alpha_s^2)$  of Fig. 2. It is interesting to observe that, before the appearance of the  $\mathcal{O}(\alpha\alpha_s^2)$  corrections in Eq. (1) [11,22], the uncertainty due to the lack of these terms could have been estimated from the scale variation of the  $\mathcal{O}(\alpha\alpha_s)$  OS ( $\overline{\text{MS}}$ ) calculation with  $\xi_{max} = 4$  (2.1). Thus, we may expect that similar scale variations will also yield meaningful results in the next order.

The separation of  $\mu_c$  and  $\mu_m$  is perhaps not so easy to motivate on physical grounds. In Fig. 4, we analyze the scale dependence of the  $\overline{\text{MS}}$  calculation of  $M_W$  to  $\mathcal{O}(\alpha\alpha_s)$  and  $\mathcal{O}(\alpha\alpha_s^2)$  identifying  $\mu_c = \mu_m = \xi\bar{\mu}_t$ . We observe that the  $\mathcal{O}(\alpha\alpha_s)$  analysis is very unstable for  $\xi \ll 1$ . For  $\xi = 1/8$ , we have  $M_W = 80.256$  GeV (see Table 3), which is way below the  $M_W$  range considered in Fig. 4. On the other hand, the  $\mathcal{O}(\alpha\alpha_s^2)$  curve nicely oscillates around the  $M_W$  value at  $\xi = 1$ , with a band-width of 13.5 MeV. In this one-dimensional analysis, the PMS points appear at  $\xi = 1.601$  in  $\mathcal{O}(\alpha\alpha_s)$  and at  $\xi = 0.280$  and  $\xi = 2.898$  in  $\mathcal{O}(\alpha\alpha_s^2)$ . They are indicated by “o” in the contour plots of Fig. 3. There is one point of FAC within Fig. 4, at

Table 4: Maximum deviations (in MeV) of the  $M_W$  values predicted for  $M_t = 180$  GeV and  $M_H = 300$  GeV via  $\Delta r$  to  $\mathcal{O}(\alpha\alpha_s)$  and  $\mathcal{O}(\alpha\alpha_s^2)$  in the OS and  $\overline{\text{MS}}$  schemes with  $1/\xi_{max} \leq \xi_c, \xi_m \leq \xi_{max}$  from the respective values for  $\xi_c = \xi_m = 1$ .

$\log_2 \xi_{max}$	$\Delta M_W$ [MeV]			
	$\mathcal{O}(\alpha_s)$ OS	$\mathcal{O}(\alpha_s)$ $\overline{\text{MS}}$	$\mathcal{O}(\alpha_s^2)$ OS	$\mathcal{O}(\alpha_s^2)$ $\overline{\text{MS}}$
1/2	+2.5	+4.5	+1.2	+1.9
	-2.8	-5.2	-1.1	-2.4
1	+4.9	+11.4	+2.4	+3.6
	-5.8	-14.4	-2.1	-5.0
3/2	+7.0	+20.8	+3.7	+5.3
	-9.0	-28.6	-2.9	-7.4
2	+9.1	+32.9	+5.0	+6.9
	-12.6	-49.4	-3.4	-10.0
5/2	+10.9	+48.0	+6.2	+8.4
	-16.6	-78.6	-3.6	-12.8
3	+12.7	+66.5	+7.5	+9.8
	-21.0	-118.8	-3.6	-16.0

$\xi = 0.413$ . Another one is located at  $\xi = 8.358$ . The BLM criterion only applies to  $\mu_c$ , but not to  $\mu_m$ , so that its implementation in our  $\overline{\text{MS}}$  analysis is ambiguous [35].

## 4 Conclusions

In this paper, we have extended an existing calculation of  $\Delta r$  in the OS scheme [2,3] to next-to-leading order in QCD by incorporating new three-loop results [11,22]. We have then converted this analysis to the  $\overline{\text{MS}}$  scheme of quark-mass renormalization in QCD. Armed with these results, we have analyzed the scheme and scale dependences of the  $M_W$  value predicted for given values of  $M_t$  (pole mass) and  $M_H$ . We have verified that both scheme and scale dependences are considerably reduced if the next-to-leading-order QCD corrections are taken into account. For  $M_t = 180$  GeV and  $M_H = 300$  GeV, the scheme dependence at the central renormalization point,  $\xi_c = \xi_m = 1$ , is reduced from 7.5 MeV to 4.8 MeV (see Table 1 and Fig. 1). The scale dependences within the interval  $1/4 \leq \xi_c, \xi_m \leq 4$  are decreased from 21.7 MeV to 8.4 MeV in the OS scheme and from 82.2 MeV to 16.9 MeV in the  $\overline{\text{MS}}$  scheme (see Tables 2, 3, 4 and Figs. 2, 3).

Although the numbers presented here are uniquely determined by the generally accepted rules of perturbation theory, their interpretation in terms of a QCD-related theoretical un-

certainty in  $M_W$  allows for a certain amount freedom. Nevertheless, we shall propose an algorithm to extract a central value and an error of  $M_W$ . If we adopt the point of view that the OS and  $\overline{\text{MS}}$  analyses represent two independent theoretical determinations of  $M_W$  with their individual errors, then we may combine them assuming Gaussian statistics as we usually do with independent experimental measurements [26]. It is plausible and conservative to identify the error in each scheme with the absolute of the maximum deviation of  $M_W$  in the interval  $1/\xi_{max} \leq \xi_c, \xi_m \leq \xi_{max}$  from the central value, at  $\xi_c = \xi_m = 1$ . This will leave room for the reader to select his preferred value of  $\xi_{max}$ . For illustration, we shall again assume that  $M_t = 180$  GeV and  $M_H = 300$  GeV. The OS and  $\overline{\text{MS}}$  central values of  $M_W$  and the respective errors may then be read off from Tables 2, 3, and 4. For  $\xi_{max} = 4$ , we so obtain  $(80.367 \pm 0.012)$  GeV to  $\mathcal{O}(\alpha\alpha_s)$  and  $(80.355 \pm 0.004)$  GeV to  $\mathcal{O}(\alpha\alpha_s^2)$ . We would like to point out that the  $\mathcal{O}(\alpha\alpha_s^2)$  central value is encompassed by the  $\mathcal{O}(\alpha\alpha_s)$  error, and that, in each order, the OS and  $\overline{\text{MS}}$  central values lie within the error. This reassures us of the soundness of our procedure. The corresponding results for other values of  $\xi_{max}$  may be seen from Fig. 5. It is clear that this approach does not make sense if  $\xi_{max}$  is so small that the scale variations of the OS and  $\overline{\text{MS}}$  calculations do not overlap.

Apart from the theoretical uncertainty due to the lack of knowledge of QCD corrections to  $\Delta r$  beyond three loops, which we have estimated here, there is another source of QCD-related error, namely the one connected with  $\Delta\alpha_{had}^{(5)}$ , which is extracted from experimental data of  $e^+e^- \rightarrow hadrons$  via a dispersion relation [28,36]. In Ref. [28], this error has been estimated to be  $\pm 0.0007$ , which, for  $M_t = (180 \pm 12)$  GeV and  $60 \text{ GeV} \leq M_H \leq 1 \text{ TeV}$ , translates into an error of approximately  $\pm 13$  MeV in  $M_W$ . Other recent determinations of  $\Delta\alpha_{had}^{(5)}$  [36] agree with the result of Ref. [28] within less than two standard deviations of the latter.

Finally, we would like to mention that the lack of knowledge of three-loop and subleading two-loop electroweak corrections to  $\Delta r$  represents another source of theoretical error on the  $M_W$  determination from the measured muon lifetime. The magnitude of the recently calculated  $\mathcal{O}(G_F^2 M_t^2 M_W^2)$  correction to  $\Delta\rho$  [37] indicates that the still uncontrolled  $\mathcal{O}(G_F^2 M_t^2 M_W^2)$  term of  $\Delta r$  might have the potential to jeopardize the accuracy of the indirect  $M_W$  determination. The study of the scheme and scale dependences of the dominant two-loop electroweak corrections provides us with a clue to the size of higher-order electroweak effects [38].

## ACKNOWLEDGEMENTS

I am grateful to Bill Bardeen for carefully reading the manuscript, to Gerhard Buchalla for a useful comment on the separation of coupling and mass renormalization scales, to Kostja Chetyrkin for making available to me the results of Ref. [22] in algebraic form, to Paul Mackenzie for a helpful conversation about Ref. [33], to Sergei Larin and Levan Surguladze for clarifying communications regarding the decoupling relation [39], and to Alberto Sirlin for illuminating discussions concerning the scheme and scale dependences of  $\Delta\rho$ . I am indebted

to the FNAL Theory Group for inviting me as a Guest Scientist and for the great hospitality extended to me.

## A Appendix

In this Appendix, we shall provide a few general relations which are useful for implementing the  $\mu$  dependence of the QCD coupling constant and the quark masses in the  $\overline{\text{MS}}$  scheme. We shall take the colour gauge group to be  $\text{SU}(N_c)$ ;  $C_F = (N_c^2 - 1)/(2N_c)$  and  $C_A = N_c$  are the Casimir operators of its fundamental and adjoint representations, respectively, and  $T_F = 1/2$  is the trace normalization of its fundamental representation. We shall keep the number of active quark flavours,  $n_f$ , arbitrary. The RG equations for the so-called couplant,  $a(\mu) = \alpha_s(\mu)/\pi$ , and  $m(\mu)$  may be found, *e.g.*, in Ref. [39]. For the reader's convenience, we list them here:

$$\frac{da}{d \ln \mu} = \beta(a) = -a^2 [\beta_0 + \beta_1 a + \beta_2 a^2 + \mathcal{O}(a^3)], \quad (18)$$

$$\frac{d \ln m}{d \ln \mu} = -\gamma_m(a) = -a [\gamma_0 + \gamma_1 a + \gamma_2 a^2 + \mathcal{O}(a^3)], \quad (19)$$

where [40]

$$\begin{aligned} \beta_0 &= \frac{1}{4} \left( \frac{11}{3} C_A - \frac{4}{3} T_F n_f \right), \\ \beta_1 &= \frac{1}{16} \left( \frac{34}{3} C_A^2 - 4 C_F T_F n_f - \frac{20}{3} C_A T_F n_f \right), \\ \beta_2 &= \frac{1}{64} \left( \frac{2857}{54} C_A^3 + 2 C_F^2 T_F n_f - \frac{205}{9} C_F C_A T_F n_f - \frac{1415}{27} C_A^2 T_F n_f + \frac{44}{9} C_F T_F^2 n_f^2 \right. \\ &\quad \left. + \frac{158}{27} C_A T_F^2 n_f^2 \right) \end{aligned} \quad (20)$$

are the first three coefficients of the Callan-Symanzik beta function and [20,41]

$$\begin{aligned} \gamma_0 &= \frac{3}{4} C_F, \\ \gamma_1 &= \frac{1}{16} \left( \frac{3}{2} C_F^2 + \frac{97}{6} C_F C_A - \frac{10}{3} C_F T_F n_f \right), \\ \gamma_2 &= \frac{1}{64} \left\{ \frac{129}{2} C_F^3 - \frac{129}{4} C_F^2 C_A + \frac{11413}{108} C_F C_A^2 + C_F^2 T_F n_f [48\zeta(3) - 46] \right. \\ &\quad \left. + C_F C_A T_F n_f \left[ -48\zeta(3) - \frac{556}{27} \right] - \frac{140}{27} C_F T_F^2 n_f^2 \right\} \end{aligned} \quad (21)$$

are the first three coefficients of the quark-mass anomalous dimension. Here,  $\zeta$  is Riemann's zeta function, with value  $\zeta(3) \approx 1.202\,057$ . Our aim is to evaluate  $a = a(\mu)$  and  $m = m(\mu)$  for  $\mu$  arbitrary, assuming that their values,  $a_0 = a(\mu_0)$  and  $m_0 = m(\mu_0)$ , are known at some starting scale,  $\mu_0$ .

Beyond the leading order, Eq. (18) cannot be exactly solved for  $a$ . A perturbative solution reads

$$a = a_0 \left[ 1 - a_0 \beta_0 \ell + a_0^2 \ell (\beta_0^2 \ell - \beta_1) + a_0^3 \ell \left( -\beta_0^3 \ell^2 + \frac{5}{2} \beta_0 \beta_1 \ell - \beta_2 \right) + \mathcal{O}(a_0^4 \ell^4) \right], \quad (22)$$

where  $\ell = \ln(\mu^2/\mu_0^2)$ . The leading logarithms in Eq. (22) may be resummed by writing [42]

$$a = \frac{a_0}{1 + a_0 \ell [\beta_0 + a_0 \beta_1 + a_0^2 (-\beta_0 \beta_1 \ell / 2 + \beta_2)]}. \quad (23)$$

We recover the exact leading-order solution of Eq. (18) by discarding the terms of  $\mathcal{O}(a_0^2)$  in the denominator of Eq. (23).

Knowing the  $\mu$  dependence of  $a$ , it is sufficient to obtain  $m$  as a function of  $a$ . Dividing Eq. (19) by Eq. (18), we obtain a differential equation which may be exactly solved for  $m$ , given the coefficients of  $\beta$  and  $\gamma_m$  to a certain order. The exact solutions to leading and next-to-leading orders read

$$m = m_0 \left( \frac{a}{a_0} \right)^{\gamma_0/\beta_0}, \quad (24)$$

$$m = m_0 \left( \frac{a}{a_0} \right)^{\gamma_0/\beta_0} \left( \frac{\beta_0 + a \beta_1}{\beta_0 + a_0 \beta_1} \right)^{\gamma_1/\beta_1 - \gamma_0/\beta_0}, \quad (25)$$

respectively. A perturbative solution of Eq. (19) similar to Eq. (22) is given by

$$m = m_0 \left\{ 1 - a_0 \gamma_0 \ell + a_0^2 \ell \left[ \frac{\gamma_0}{2} (\beta_0 + \gamma_0) \ell - \gamma_1 \right] + a_0^3 \ell \left[ -\gamma_0 \left( \frac{\beta_0^2}{3} + \frac{\beta_0 \gamma_0}{2} + \frac{\gamma_0^2}{6} \right) \ell^2 + \left( \beta_0 \gamma_1 + \frac{\beta_1 \gamma_0}{2} + \gamma_0 \gamma_1 \right) \ell - \gamma_2 \right] + \mathcal{O}(a_0^4 \ell^4) \right\}, \quad (26)$$

where  $\ell$  is defined below Eq. (22). By iterating Eq. (26), we may generate a closed expression for the mass parameter  $\bar{m} = m(\bar{\mu})$  in terms of  $a$  and  $m$  for  $\mu$  arbitrary:

$$\bar{m} = m \left\{ 1 + a \gamma_0 \ell + a^2 \ell \left[ \frac{\gamma_0}{2} (\beta_0 + \gamma_0) \ell - 2\gamma_0^2 + \gamma_1 \right] + a^3 \ell \left[ \gamma_0 \left( \frac{\beta_0^2}{3} + \frac{\beta_0 \gamma_0}{2} + \frac{\gamma_0^2}{6} \right) \ell^2 + \left( -3\beta_0 \gamma_0^2 + \beta_0 \gamma_1 + \frac{\beta_1 \gamma_0}{2} - 2\gamma_0^3 + \gamma_0 \gamma_1 \right) \ell + 4\gamma_0^3 - 4\gamma_0 \gamma_1 + \gamma_2 \right] + \mathcal{O}(a^4 \ell^4) \right\}, \quad (27)$$

where  $l = \ln(\mu^2/m^2)$ . The right-hand side of Eq. (27) is manifestly RG invariant through  $\mathcal{O}(a^3)$ .

In the remainder of this section, we shall consider QCD with one massive quark and  $n_f - 1$  massless flavours. The relation between the pole mass,  $M$ , and  $m(M)$  at next-to-leading order is given by [20,43]

$$\frac{M}{m(M)} = 1 + a(M)C_F + a^2(M)K_0 + \mathcal{O}(a^3), \quad (28)$$

where [43]

$$\begin{aligned} K_0 &= C_F \left[ \frac{3}{4}\zeta(2) - \frac{3}{8} \right] + C_F^2 \left[ \frac{3}{4}\zeta(3) + \zeta(2) \left( -3\ln 2 + \frac{15}{8} \right) + \frac{121}{128} \right] \\ &\quad + C_F C_A \left[ -\frac{3}{8}\zeta(3) + \zeta(2) \left( \frac{3}{2}\ln 2 - \frac{1}{2} \right) + \frac{1111}{384} \right] + C_F n_f \left[ -\frac{\zeta(2)}{4} - \frac{71}{192} \right] \\ &\approx 17.151\,430 - 1.041\,367\,n_f. \end{aligned} \quad (29)$$

Here,  $\zeta(2) = \pi^2/6$  and the value of  $\zeta(3)$  is listed below Eq. (21). Using Eq. (28) along with Eqs. (22) and (26), we may express  $M$  entirely in terms of  $\overline{\text{MS}}$  parameters, viz.

$$\begin{aligned} M &= m \left\{ 1 + a(\gamma_0 l + C_F) + a^2 \left[ \frac{\gamma_0}{2}(\beta_0 + \gamma_0)l^2 + (-2\gamma_0^2 + \gamma_1 + C_F(\beta_0 + \gamma_0))l - 2\gamma_0 C_F \right. \right. \\ &\quad \left. \left. + K_0 \right] + \mathcal{O}(a^3 l^3) \right\}, \end{aligned} \quad (30)$$

where  $l$  is defined below Eq. (27). The right-hand side of Eq. (30) is RG invariant through  $\mathcal{O}(a^2)$  as it must be. Substituting Eq. (28) into Eq. (27) evaluated at  $\mu = M$ , we obtain a closed expression of  $\bar{\mu}$  in terms of  $M$  [44],

$$\bar{\mu} = M \left\{ 1 - a(M)C_F + a^2(M) [C_F(2\gamma_0 + C_F) - K_0] + \mathcal{O}(a^3) \right\}. \quad (31)$$

In Eqs. (28), (30), and (31),  $a$  refers to  $n_f$  quark flavours, *i.e.*,  $a = a^{(n_f)}$ . Finally, we list the matching condition for  $a$  at the heavy-flavour threshold,  $\mu = M$ . It follows from the decoupling relation found in Ref. [39] and reads

$$a^{(n_f)}(M) = a^{(n_f-1)}(M) \left\{ 1 + [a^{(n_f-1)}(M)]^2 T_F \left( \frac{15}{16}C_F - \frac{2}{9}C_A \right) + \mathcal{O}(a^3) \right\}. \quad (32)$$

## References

- [1] F. Halzen and B.A. Kniehl, Nucl. Phys. **B353**, 567 (1991).



- [2] F. Halzen, B.A. Kniehl, and M.L. Stong, in *Particle Physics: VI Jorge André Swieca Summer School*, Campos de Jordão, Brasil, 14–26 January, 1991, edited by O.J.P. Éboli, M. Gomes, and A. Santoro (World Scientific, Singapore, 1992) p. 219; *Z. Phys. C* **58**, 119 (1993).
- [3] S. Fanchiotti, B. Kniehl, and A. Sirlin, *Phys. Rev. D* **48**, 307 (1993).
- [4] G. Altarelli, R. Barbieri, and S. Jadach, *Nucl. Phys.* **B369**, 3 (1992); Z. Hioki, *Phys. Rev. D* **45**, 1814 (1992); *Mod. Phys. Lett. A* **7**, 1009 (1992); *Phys. Lett. B* **340**, 181 (1994); J. Ellis, G.L. Fogli, and E. Lisi, *Phys. Lett. B* **274**, 456 (1992); *Phys. Lett. B* **285**, 238 (1992); *Phys. Lett. B* **292**, 427 (1992); *Phys. Lett. B* **318**, 148 (1993); *Phys. Lett. B* **324**, 173 (1994); *Phys. Lett. B* **333**, 118 (1994); F. Halzen, P. Roy, and M.L. Stong, *Phys. Lett. B* **277**, 503 (1992); F. del Aguila, M. Martínez, and M. Quirós, *Nucl. Phys.* **B381**, 451 (1992); V.A. Novikov, L.B. Okun, and M.I. Vysotsky, *Phys. Lett. B* **299**, 329 (1993); **304**, 386(E) (1993); G. Altarelli, R. Barbieri, and F. Caravaglios, *Nucl. Phys.* **B405**, 3 (1993); *Phys. Lett. B* **349**, 145 (1995); V.A. Novikov, L.B. Okun, M.I. Vysotsky, and V.P. Yurov, *Phys. Lett. B* **308**, 123 (1993); G. Passarino, *Phys. Lett. B* **313**, 213 (1993); *Z. Phys. C* **62**, 229 (1994); N.A. Nekrasov, V.A. Novikov, L.B. Okun, and M.I. Vysotsky, *Yad. Fiz.* **57**, 883 (1994) [*Phys. Atom. Nucl.* **57**, 827 (1994)]; V.A. Novikov, L.B. Okun, A.N. Rozanov, and M.I. Vysotsky, *Phys. Lett. B* **331**, 433 (1994); *Mod. Phys. Lett. A* **9**, 2641 (1994); G. Montagna, O. Nicrosini, G. Passarino, and F. Piccinini, *Phys. Lett. B* **335**, 484 (1994); Z. Hioki and R. Najima, *Mod. Phys. Lett. A* **10**, 121 (1995); K. Hagiwara, D. Haidt, C.S. Kim, and S. Matsumoto, *Z. Phys. C* **64**, 559 (1994); M. Consoli and Z. Hioki, *Mod. Phys. Lett. A* **10**, 845 (1995); Report Nos. TOKUSHIMA 95–03 and hep-ph/9505249 (May 1995).
- [5] T.H. Chang, K.J.F. Gaemers, and W.L. van Neerven, *Phys. Lett.* **108B**, 222 (1982); *Nucl. Phys.* **B202**, 407 (1982).
- [6] A. Djouadi and C. Verzegnassi, *Phys. Lett. B* **195**, 265 (1987); A. Djouadi, *Nuovo Cim.* **100A**, 357 (1988).
- [7] B.A. Kniehl, *Nucl. Phys.* **B347**, 86 (1990).
- [8] A. Djouadi and P. Gambino, *Phys. Rev. D* **49**, 3499 (1994); *Phys. Rev. D* **49**, 4705 (1994).
- [9] CDF Collaboration, F. Abe *et al.*, *Phys. Rev. Lett.* **74**, 2626 (1995); D0 Collaboration, S. Abachi *et al.*, *Phys. Rev. Lett.* **74**, 2632 (1995).
- [10] D.A. Ross and M. Veltman, *Nucl. Phys.* **B95**, 135 (1975); M. Veltman, *Nucl. Phys.* **B123**, 89 (1977).

- [11] L. Avdeev, J. Fleischer, S. Mikhailov, and O. Tarasov, Phys. Lett. B **336**, 560 (1994); **349**, 597(E) (1995); K.G. Chetyrkin, J.H. Kühn, and M. Steinhauser, Phys. Lett. B **351**, 331 (1995); in *Proceedings of the Ringberg Workshop on Perspectives of Electroweak Interactions in  $e^+e^-$  Collisions*, Tegernsee, Germany, February 5–8, 1995, edited by B.A. Kniehl (World Scientific, Singapore, 1995).
- [12] A. Sirlin, Phys. Rev. D **22**, 971 (1980).
- [13] W.A. Bardeen, A.J. Buras, D.W. Duke, and T. Muta, Phys. Rev. D **18**, 3998 (1978).
- [14] B.A. Kniehl and A. Sirlin, Phys. Rev. D **47**, 883 (1993); B.A. Kniehl, Phys. Rev. D **51**, 3803 (1995).
- [15] F.J. Ynduráin, Phys. Lett. B **321**, 400 (1994) [The results of this letter are revised by K. Adel and F.J. Ynduráin, Madrid University Report No. FTUAM 95–2, hep-ph/9502290 (February 1995).]; M.C. Gonzalez-Garcia, F. Halzen, and R.A. Vázquez, Phys. Lett. B **322**, 233 (1994).
- [16] B.A. Kniehl, in *Reports of the Working Group on Precision Calculations for the Z Resonance*, edited by D.Yu. Bardin, W. Hollik, and G. Passarino, CERN Yellow Report No. 95–03 (March 1995) p. 299.
- [17] K-I. Aoki, Z. Hioki, R. Kawabe, M. Konuma, and T. Muta, Prog. Theor. Phys. Suppl. **73**, 1 (1982); M. Böhm, H. Spiesberger, and W. Hollik, Fortschr. Phys. **34**, 687 (1986).
- [18] B.A. Kniehl, J.H. Kühn, and R.G. Stuart, Phys. Lett. B **214**, 621 (1988).
- [19] B.A. Kniehl and A. Sirlin, Phys. Lett. B **318**, 367 (1993); B.A. Kniehl, Phys. Rev. D **50**, 3314 (1994).
- [20] R. Tarrach, Nucl. Phys. **B183**, 384 (1981).
- [21] B.A. Kniehl and J.H. Kühn, Nucl. Phys. **B329**, 547 (1990).
- [22] K.G. Chetyrkin, J.H. Kühn, and M. Steinhauser, Report Nos. SLAC-PUB-95-6851, TTP95-13, and hep-ph/9504413 (April 1995); K.G. Chetyrkin, private communication.
- [23] F. Jegerlehner, in *Progress in Particle and Nuclear Physics*, edited by A. Faessler (Pergamon Press, Oxford, 1991) Vol. 27, p. 1.
- [24] R. Barbieri, M. Beccaria, P. Ciafaloni, G. Curci, and A. Viceré, Phys. Lett. B **288**, 95 (1992); **313**, 511(E) (1993); Nucl. Phys. **B409**, 105 (1993); J. Fleischer, O.V. Tarasov, and F. Jegerlehner, Phys. Lett. B **319**, 249 (1993); Phys. Rev. D **51**, 3820 (1995).

- [25] R. Barbieri, P. Ciafaloni, and A. Strumia, *Phys. Lett. B* **317**, 381 (1993).
- [26] Particle Data Group, L. Montanet *et al.*, *Phys. Rev. D* **50**, 1173 (1994).
- [27] M.G. Alviggi *et al.* (LEP Electroweak Working Group), Report Nos. LEPEWWG/95–01, ALEPH 95–038 PHYSIC 95–036, DELPHI 95–37 PHYS 482, L3 Note 1736, OPAL Technical Note TN284 (March 1995).
- [28] S. Eidelman and F. Jegerlehner, Report Nos. PSI–PR–95–1, BudkerINP 95–5, hep–ph/9502298 (January 1995).
- [29] S. Bethke, in *Proceedings of the Tennessee International Symposium on Radiative Corrections: Status and Outlook*, Gatlinburg, Tennessee, June 27–July 1, 1994, edited by B.F.L. Ward (World Scientific, Singapore, 1994).
- [30] P.M. Stevenson, *Phys. Rev. D* **23**, 2916 (1981); *Phys. Lett.* **100B**, 61 (1981); *Nucl. Phys.* **B203**, 472 (1982); *Nucl. Phys.* **B231**, 65 (1984).
- [31] G. Grunberg, *Phys. Lett.* **95B**, 70 (1980); **110B**, 501(E) (1982); *Phys. Rev. D* **29**, 2315 (1984).
- [32] A. Sirlin, *Phys. Lett. B* **348**, 201 (1995); **352**, 498(A) (1995); K. Philippides and A. Sirlin; Report Nos. NYU–TH–95/03/01 and hep–ph/9503434 (March 1995), *Nucl. Phys. B* (in press).
- [33] S.J. Brodsky, G.P. Lepage, and P.B. Mackenzie, *Phys. Rev. D* **28**, 228 (1983).
- [34] B.H. Smith and M.B. Voloshin, *Phys. Rev. D* **51**, 5251 (1995).
- [35] P.B. Mackenzie, private communication.
- [36] M.L. Swartz, Report Nos. SLAC–PUB–6710 and hep–ph/9411353 (November 1994), submitted to *Phys. Rev. D*; A.D. Martin and D. Zeppenfeld, *Phys. Lett. B* **345**, 558 (1995).
- [37] G. Degrassi, S. Fanchiotti, and P. Gambino, *Int. J. Mod. Phys. A* **10**, 1337 (1995); G. Degrassi, S. Fanchiotti, F. Feruglio, P. Gambino, and A. Vicini, *Phys. Lett. B* **350**, 75 (1995); Report Nos. DFPD 95/TH/29 and hep–ph/9507286 (July 1995), to appear in *Proceedings of the XXXth Rencontre de Moriond: Electroweak Interactions and Unified Theories*, Les Arcs, France, March 11–18, 1995, edited by J. Trân Thanh Vân (Editions Frontières, Gif-sur-Yvette, 1995).
- [38] A.I. Bochkarev and R.S. Willey, *Phys. Rev. D* **51**, R2049 (1995); B.A. Kniehl and A. Sirlin, in preparation.

- [39] S.A. Larin, T. van Ritbergen, and J.A.M. Vermaseren, Nucl. Phys. **B438**, 278 (1995).
- [40] D.J. Gross and F. Wilczek, Phys. Rev. Lett. **30**, 1343 (1973); Phys. Rev. D **8**, 3633 (1973); H.D. Politzer, Phys. Rev. Lett. **30**, 1346 (1973); D.R.T. Jones, Nucl. Phys. **B75**, 531 (1974); W.E. Caswell, Phys. Rev. Lett. **33**, 244 (1974); O.V. Tarasov, A.A. Vladimirov, and A.Yu. Zharkov, Phys. Lett. **93B**, 429 (1980); S.A. Larin and J.A.M. Vermaseren, Phys. Lett. B **303**, 334 (1993).
- [41] O. Nachtmann and W. Wetzel, Nucl. Phys. **B187**, 333 (1981); O.V. Tarasov, Dubna Report No. JINR P2-82-900 (1982).
- [42] W.T. Giele, E.W.N. Glover, and J. Yu, FNAL Report Nos. FERMILAB-Pub-95/127-T, DTP/95/52, and hep-ph/9506442 (June 1995); A. Sirlin, private communication.
- [43] N. Gray, D.J. Broadhurst, W. Grafe, and K. Schilcher, Z. Phys. C **48**, 673 (1990).
- [44] B.A. Kniehl and M. Steinhauser, Report Nos. FERMILAB-PUB-95/195-T, MAD/PH/894, MPI/PhT/95-64, and TTP95-27 (July 1995).

## FIGURE CAPTIONS

Figure 1: Difference (in MeV) between the  $\overline{\text{MS}}$  and OS evaluations of  $M_W$  via  $\Delta r$  to  $\mathcal{O}(\alpha\alpha_s)$  (dashed lines) and  $\mathcal{O}(\alpha\alpha_s^2)$  (solid lines) with  $\xi_c = \xi_m = 1$  as a function of  $M_H$  for  $M_t = 168, 180,$  and  $192$  GeV. Upper curves correspond to larger  $M_t$  values.

Figure 2:  $\mu_c$  dependence of the OS evaluation of  $M_W$  (in GeV) via  $\Delta r$  to  $\mathcal{O}(\alpha\alpha_s)$  (dashed line) and  $\mathcal{O}(\alpha\alpha_s^2)$  (solid line) for  $M_t = 180$  GeV and  $M_H = 300$  GeV.

Figure 3:  $\mu_c$  and  $\mu_m$  dependences of the  $\overline{\text{MS}}$  evaluation of  $M_W$  via  $\Delta r$  to (a)  $\mathcal{O}(\alpha\alpha_s)$  and (b)  $\mathcal{O}(\alpha\alpha_s^2)$  for  $M_t = 180$  GeV and  $M_H = 300$  GeV. The contours of constant deviation (in MeV) from the value at  $\xi_c = \xi_m = 1$  (marked by  $+$ ) are shown in the  $(\log_2 \xi_c, \log_2 \xi_m)$  plane. The saddle points in this plane are marked with “ $x$ ,” the maxima and minima on the diagonal  $\xi_c = \xi_m$  are marked with “ $o$ .”

Figure 4:  $\mu_c$  dependence of the  $\overline{\text{MS}}$  evaluation of  $M_W$  (in GeV) via  $\Delta r$  to  $\mathcal{O}(\alpha\alpha_s)$  (dashed line) and  $\mathcal{O}(\alpha\alpha_s^2)$  (solid line) with  $\mu_c = \mu_m$  for  $M_t = 180$  GeV and  $M_H = 300$  GeV.

Figure 5: Central values and QCD-related errors of  $M_W$  (in GeV) evaluated via  $\Delta r$  to  $\mathcal{O}(\alpha\alpha_s)$  (dashed lines) and  $\mathcal{O}(\alpha\alpha_s^2)$  (solid lines) with  $1/\xi_{max} \leq \xi_c, \xi_m \leq \xi_{max}$  for  $M_t = 180$  GeV and  $M_H = 300$  GeV as a function of  $\xi_{max}$ .

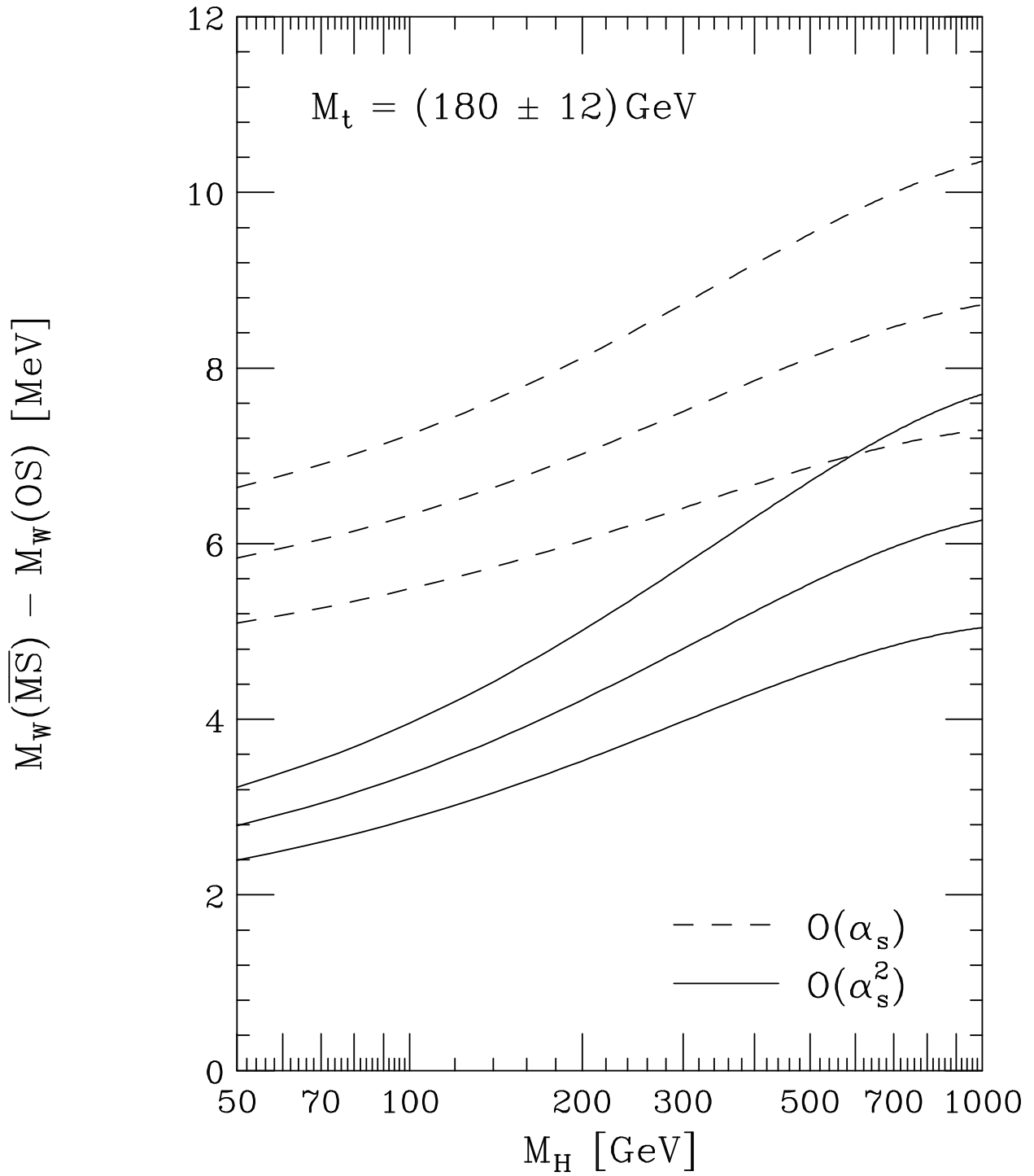


Fig. 1

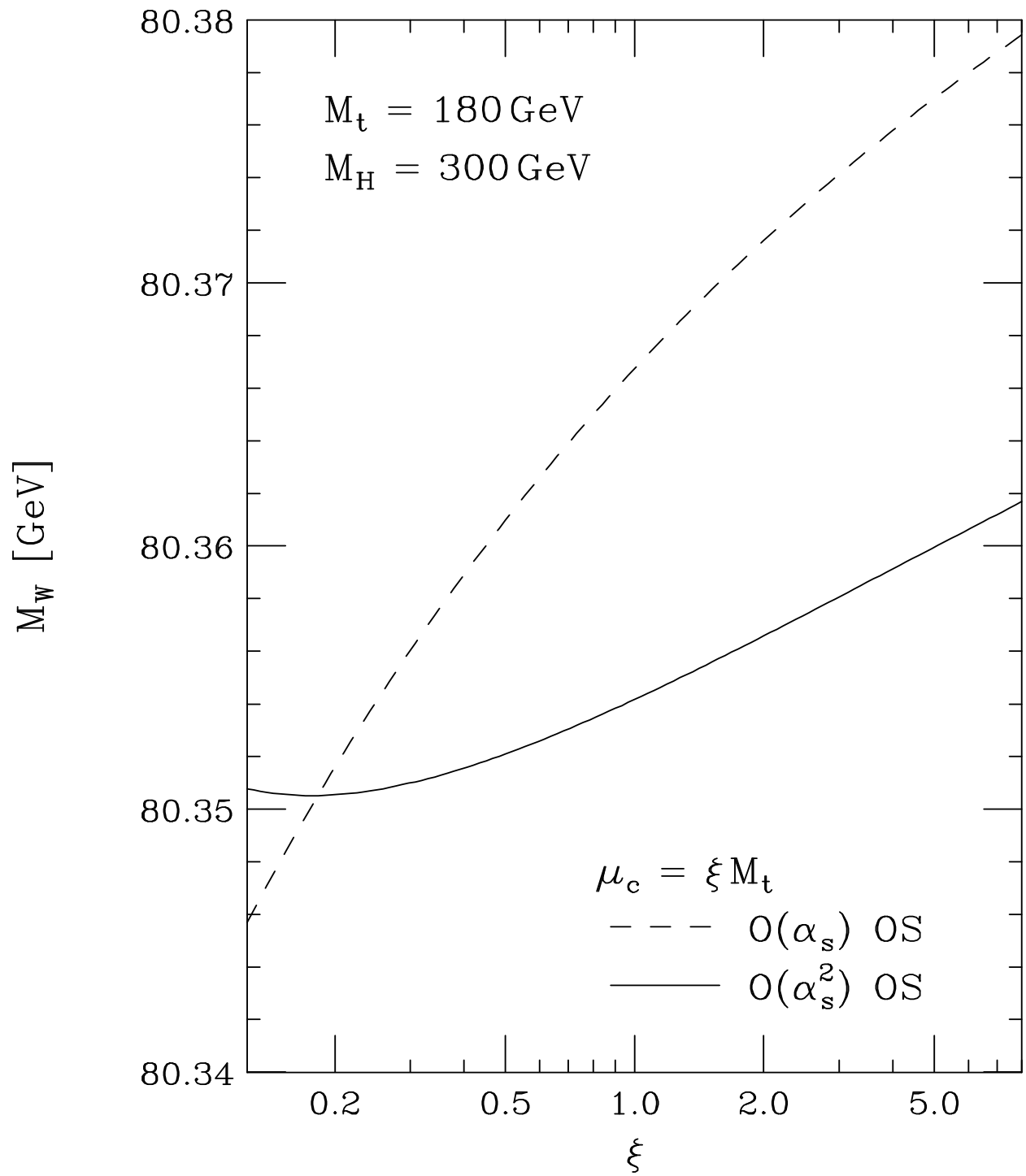
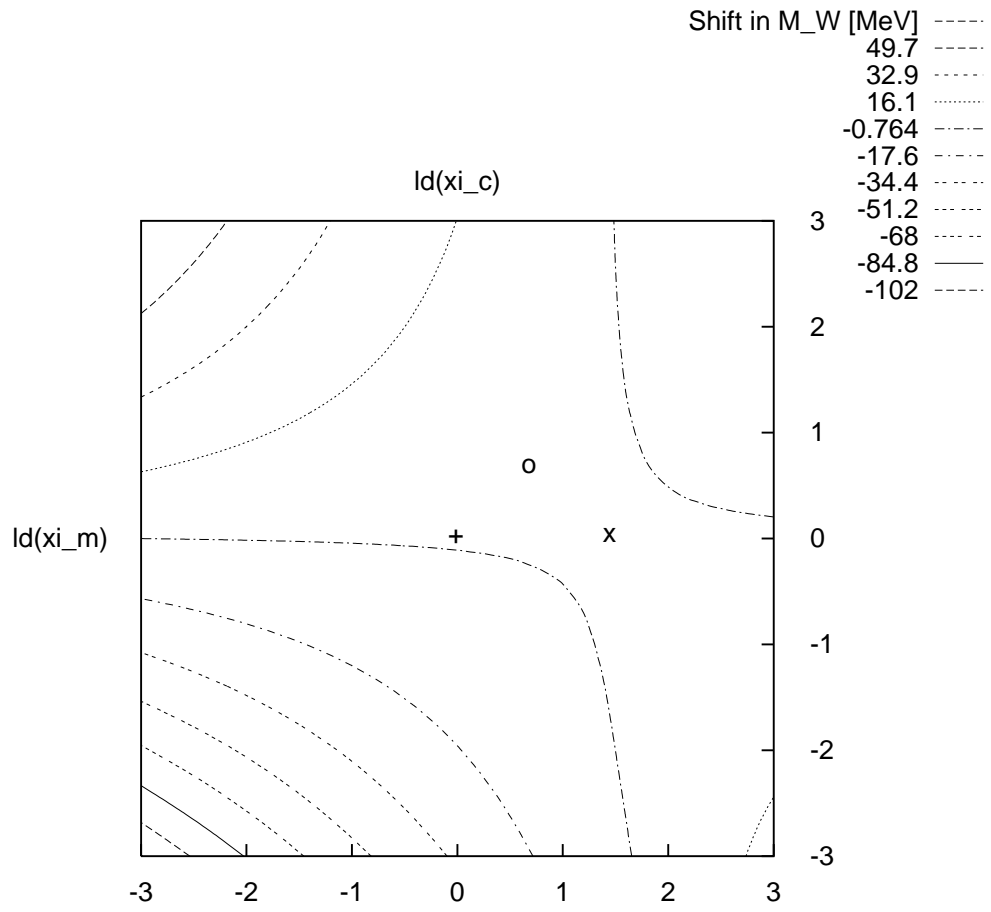
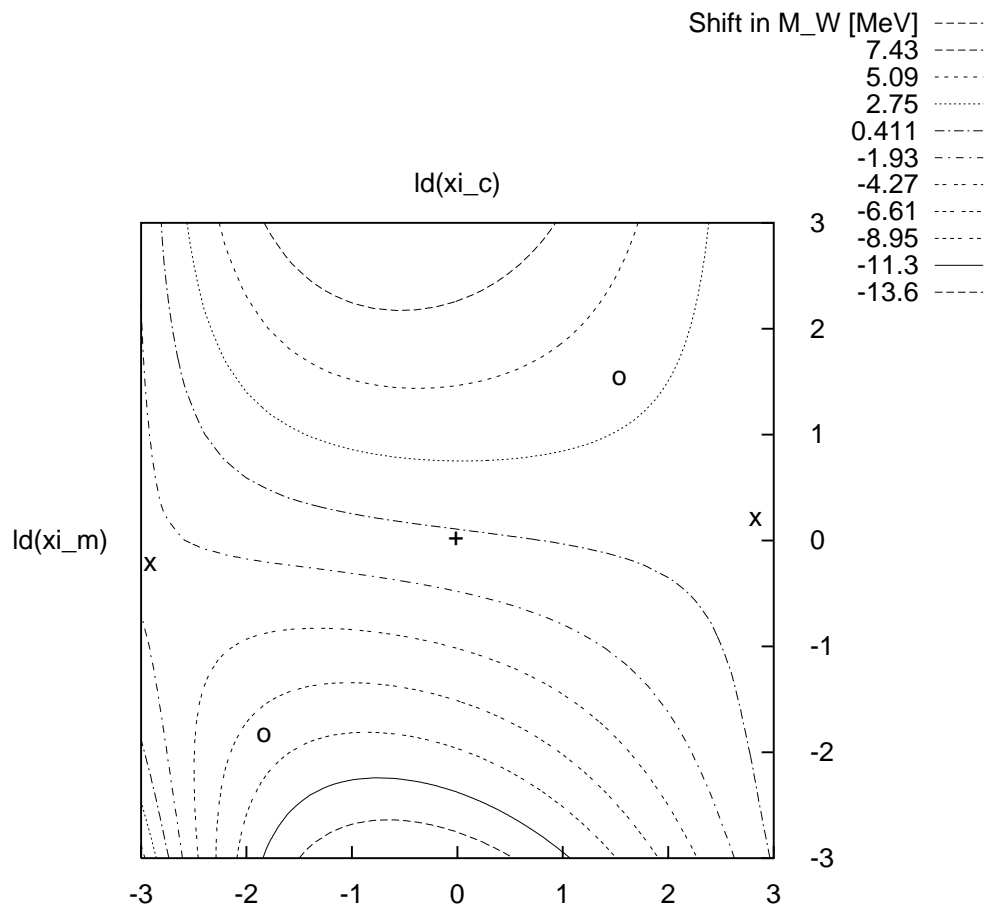


Fig. 2







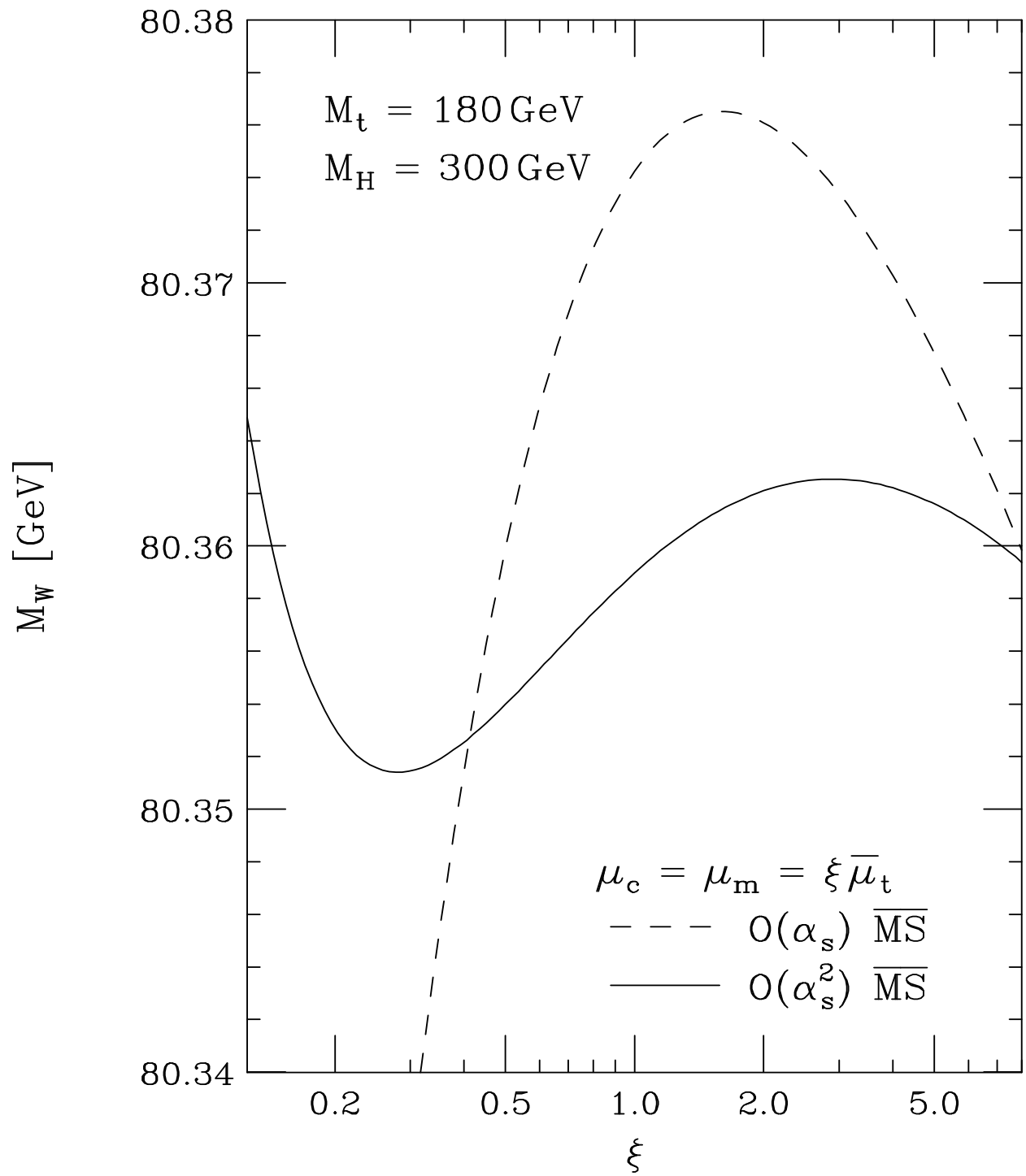


Fig. 4

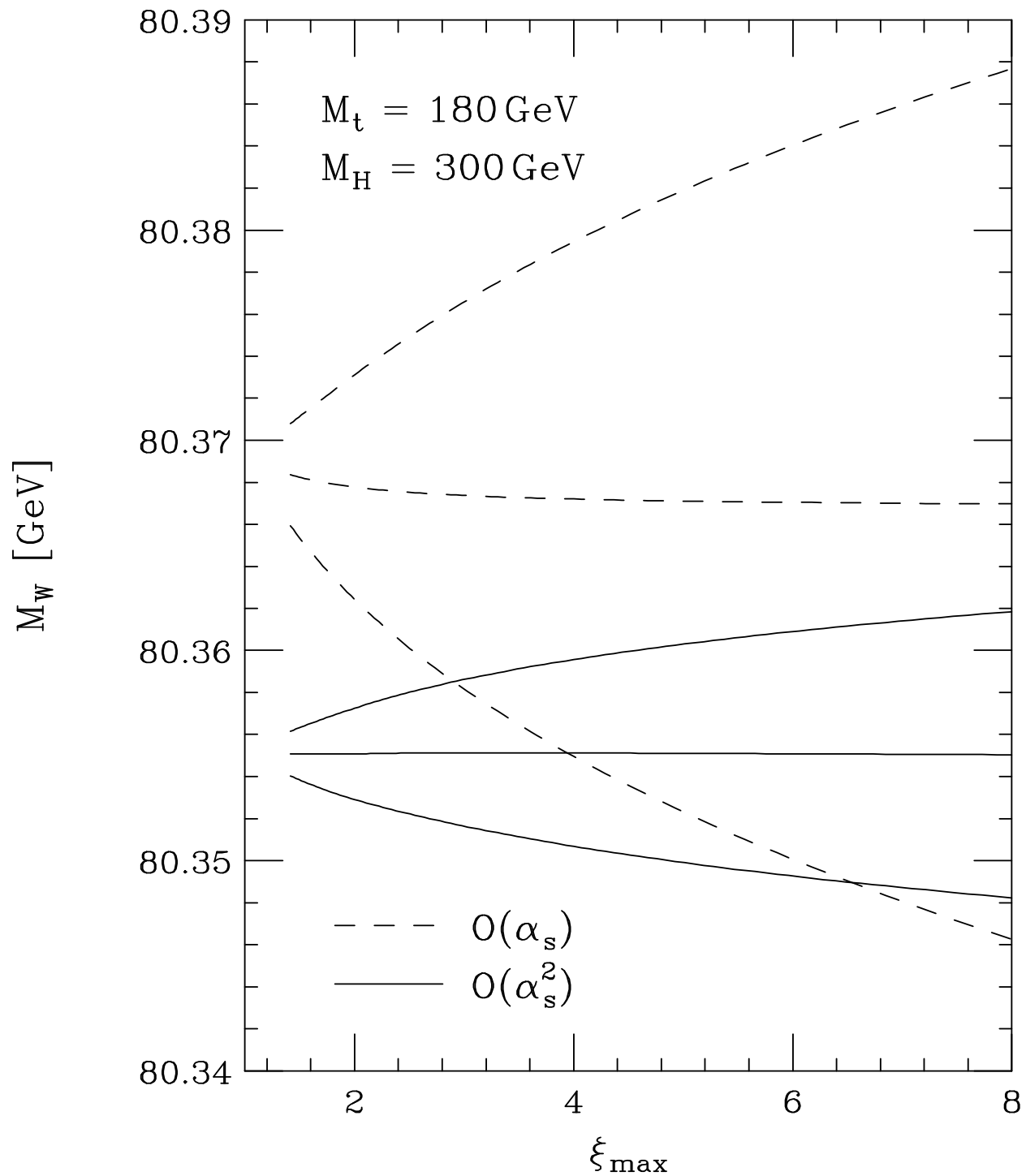


Fig. 5